JOC The Journal of Organic Chemistry

Article

pubs.acs.org/joc

Congeners of Pyrromethene-567 Dye: Perspectives from Synthesis, Photophysics, Photostability, Laser, and TD-DFT Theory

Kishor G. Thorat,[†] Priyadarshani Kamble,[‡] Ramnath Mallah,[†] Alok K. Ray,*[,‡] and Nagaiyan Sekar*[,†]

[†]Dyestuff Technology Department, Institute of Chemical Technology, Matunga, Mumbai, 400 019, India

[‡]Laser & Plasma Technology Division, Bhabha Atomic Research Centre, Mumbai, 400 085, India

Supporting Information

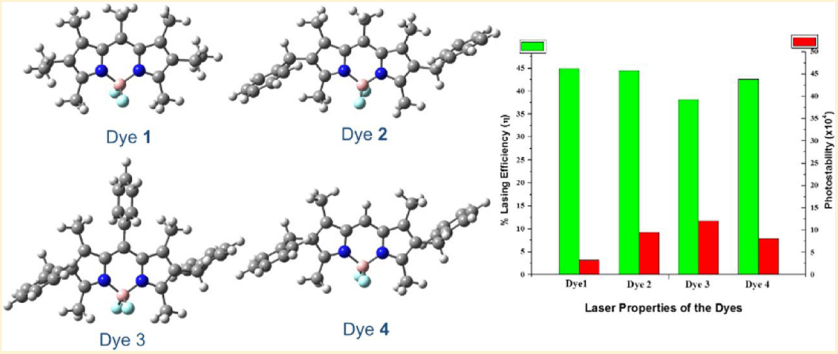

ABSTRACT: In an attempt to develop photostable and efficient BODIPY (PM) dyes for use in liquid dye lasers, three new congeners of widely used laser dye, PM567, were synthesized and their photophysical properties in various organic solvents, laser performances, and photostabilities in a selected solvent, 1,4-dioxane, have been investigated using a frequency doubled Q-switched (10 Hz) Nd:YAG laser at 532 nm. The results of photostability study in nonpolar 1,4-dioxane revealed the remarkable enhancement in stability of the novel dyes compared to that of PM567 as well as improved laser performances. Cyclic voltammetry study strongly supports the observed enhancement in photostability of the novel dyes compared to that of PM567. The observed properties of the novel dyes in relation to those of PM567 have been rationalized by extensive use of DFT and TD-DFT using the B3LYP/6-31G(d) method of theory.

INTRODUCTION

BODIPY (4,4-difluoro-4-bora-3a,4a-diaza-*s*-indacene) dyes exhibit high fluorescence quantum yields[1a,b] and can be used for such diverse applications as biolabels,[2] sensitizers in solar cells,[3] fluorescent sensors,[4a−f] molecular photonic wires,[5] and electron transfer reagents.[6]

Over the past decades, the BODIPY dyes received plenty of attention and the same is reflected in a large number of publications.[4e,f,7a−i] They exhibit low intersystem crossing (ISC) rates and low triplet extinction coefficients over the laser spectral region[1a,5,8a−e] and hence are very useful in laser applications.[9] BODIPY (also called Pyrromethene, PM) dyes exhibit good solubility in many organic solvents even in methyl methacrylate (MMA), which is useful for solid-state dye laser applications.[10a−d] In spite of the excellent photophysical and laser properties of the PM dyes, they are not yet the reliable and sustainable laser dyes for high-average power dye laser applications due to rapid photochemical degradation in normally used alcohol solvents, and they are particularly sensitive to photochemical reactions with dissolved oxygen.[11] The problem has partially been addressed by doing modifications either at the *meso* position, C-3 and/or C-5 center, or at the boron atom of the pyrromethene moiety.[12a−d]

It was envisaged that the photostabilities and lasing activities of PM dyes can be tuned by suitable modifications of the substitution pattern on the PM core.[9,12d] Earlier investigators have synthesized a host of analogues of the well-known commercial PM laser dye, PM567, by incorporating different substituents at C-8 and/or C-2 + C-6 positions (refer to Figure 1 for general structure of PM dye) of the PM moiety.[8a,13] Among these, PM650 (with CN at C-8) showed about 50 times higher photostability than PM567, but the fluorescence quantum yields of these analogues were too low to be used as laser dyes. The effect of alteration of the alkyl substituents at the pyrrole rings was found to be much less on their photochemical stabilities.[8a,13,14] It is now well-established that, under lasing conditions, the dye in its triplet state is mainly responsible for the generation of singlet oxygen; the involvement of the triplet state of the pyrromethene dye in the generation of singlet oxygen has been confirmed from their higher decomposition rates in the presence of benzophenone, a triplet sensitizer.[14] The enhanced photostability of the PM dyes in deoxygenated dye solutions and also in the presence of 1 wt

Received: March 23, 2015
Published: May 22, 2015

DOI: 10.1021/acs.joc.5b00654
J. Org. Chem. 2015, 80, 6152−6164

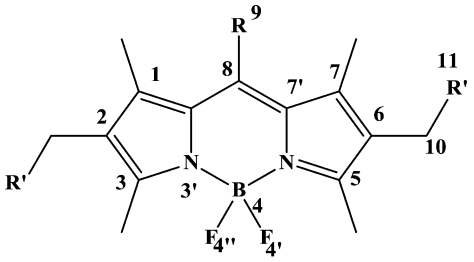

1; R=R'=Me,
2; R=Me, R'=Ph
3; R=R'=Ph
4; R=H, R'=Ph

Figure 1. Chemical structures of the BODIPY dyes under study.

% of singlet oxygen quenchers like Tin770, TBP, and DABCO confirmed the involvement of $^1O_2$ in the degradation of dye molecules, thereby decreasing the lasing efficiency over the period of longer operating time.[9] Further, singlet oxygen ($^1O_2$) reacts at the C7′−C8 double bond of the dye molecule, which produces an unstable peroxo compound, leading to the breakdown of the dye structure.[9,15] Therefore, the photostability of the PM dyes might be increased by reducing the generation of $^1O_2$ and/or their rate of reaction with $^1O_2$.

It was felt that, if one judiciously changes the substituents at either C8 or C2 + C6, the possibility of obtaining photostable PM dyes will be more compared to the commercially available known dye PM567. As far as high-average power applications of PM-based liquid dye lasers are concerned, one needs to focus more on their photochemical stability in addition to high conversion efficiency. The primary aim of the investigation was to develop a few congeners of PM567 with enhanced photostability while maintaining high dye laser efficiency by rational design.

To this end, we have synthesized the three congeners of a well-known commercially available laser dye, PM567, with the 2- and 6-positions modified using the pyrrole modified at the 3-position, the benzyl group in place of ethyl. Also, it was expected that the change in ethyl to benzyl groups at 2- and 6-positions of the PM core could alter the electrochemical properties of the PM dye to some extent, leaving photophysical properties unaltered. We have studied photophysical properties in various organic solvents, laser efficiency, and photostability properties in a selected solvent, 1,4-dioxane, of the novel PM dyes relative to that of PM567. The cyclic voltammetry study has been performed to get the idea about the electronic changes over the PM core, and the results are correlated with the observed photostabilities of the corresponding novel BODIPY dyes relative to PM567. Also, DFT and TD-DFT calculations using the B3LYP/6-31G(d) level of theory have been employed in order to get more insight on molecular structures and observed photophysical, photostability, and laser properties of the novel BODIPY dyes. The present modifications produce the positive effect on photostability and improve the laser performances of the studied dyes relative to that of widely used laser dye, PM567.[9,15] Also, maximum molar extinction coefficients of new laser dyes compared to that of PM567[10b] are found to be improved by about 2 folds on account of modifications at 2- and 6-positions of the BODIPY dyes. Thus, a lower concentration of new dyes is required for laser applications. Overall, the present modifications are found to be very useful in improving laser performances and photostabilities of the BODIPY laser dyes.

RESULTS AND DISCUSSION

Synthesis. Three novel pyrromethene laser dyes **2**−**4** (Figure 1) have been synthesized from the pyrrole in which there is a benzyl substituent at the 3-position instead of ethyl in kryptopyrrole,[15] used in the synthesis of well-known laser dye, PM567.[9,15]

The benzyl pyrrole intermediate (**9**) (Scheme 1) was obtained very easily after simple work up from its corresponding salt of carboxylic acid at room temperature as a pure solid and can be stored in a refrigerator for a few weeks. The benzyl pyrrole intermediate (**9**) (though reported by Treibs et al.[16] in 1954) and its analogues[17a,b] received negligible attention as far as synthesis and properties of BODIPY dyes. This could be because the phenyl group is not in direct conjugation with the heterocyclic pyrrole ring and would expect to produce a negligible effect on photophysical properties of typical BODIPY dyes. However, for the BODIPY as a laser dye emitting in the green-yellow region of the electromagnetic spectrum, even little changes in its electronic properties could produce a beneficial impact particularly on its photostability properties as a result of suitable modification over the PM core.[9,15] Therefore, we decided to use a benzyl pyrrole intermediate in place of commonly used kryptopyrrole for the synthesis of new BODIPY laser dyes.

Scheme 1. Synthesis of the Pyrrole Intermediate, 9

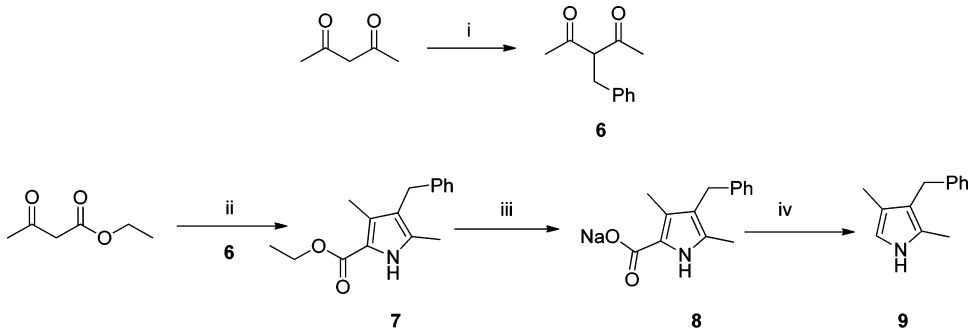

Reagents: i)Benzyl bromide/Na_2CO_3/acetone/reflux/24 h; ii)$NaNO_2$/AcOH, 0-20 ^{0}C 12 h/Zn/80 ^{0}C/1.5 h; iii)NaOH/EtOH/H_2O/reflux/5 h; iv)TFA/RT/5 min.

DOI: 10.1021/acs.joc.5b00654
J. Org. Chem. 2015, 80, 6152−6164

The dyes **2** and **3** were synthesized using the benzyl pyrrole (**9**) and the corresponding acid chlorides (Scheme 2).

Scheme 2. Synthesis of the Dyes 2 and 3

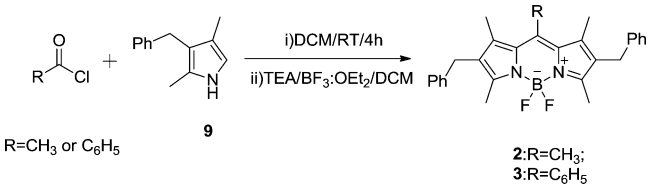

Also, we have synthesized the dye **4** by using benzyl pyrrole-2-aldehyde (**10**) with the reported protocol[18] (Scheme 3).

Photophysical Characteristics. The measured photophysical properties of the dyes **1**−**4** such as longest wavelength absorption maxima (λ_{abs}), emission maxima (λ_{em}), fluorescence quantum yields (Φ_{fl}) in solvents of various polarities and fluorescence lifetimes (τ), and calculated radiative decay (k_r) and nonradiative decay (k_{nr}) rates in selected solvents are presented in Table 1. The absorption and fluorescence spectra of the dyes **1**−**4** were recorded in various organic solvents (Table 1), but only those obtained in 1,4-dioxane are shown in Figures 2 and 3, respectively.

The PM dyes **1**−**4** in different organic solvents had intense $S_0 \rightarrow S_1$ absorption bands in the range of 518−530 nm, each with a small fwhm. Table 1 reveals that the change in solvent polarities has no or very weak influence on the absorption and emission maxima of the dyes **2**−**4**. In different organic solvents, the dye **2**, as a result of modifications at 2- and 6-positions, relative to the dye **1**, showed absorption maxima shifted hypsochromically by 1−3 nm and emission maxima shifted bathochromically by 2−3 nm, resulting in an increased Stokes shift by 3−6 nm (Table 1). The shapes of the absorption and emission spectra of the dyes **2** and **4** were similar to that of **1**, and like typical BODIPYs, they are mirror images of each other. From Figures 2 and 3 and Table 1, it can be seen that the shapes of the absorption and emission spectra of the dye **2** are very similar to that of the dye **1** with no considerable change in fwhm. The absorption and emission spectra of the dye **2** were observed to sharpen a little by 1−2 nm compared to those of the dye **1**. The dye **2** showed good fluorescence quantum yields ranging from 0.78 to 0.97 in various organic solvents (Table 1). Compared to the dye **1**, the dye **2** gave slightly decreased fluorescence lifetimes with a minimum of 4.88 ns in 1,4-dioxane and a maximum of 6.01 ns in *n*-heptane (Table 1).

The dye **3**, in which there is a phenyl group at the *meso* position along with benzyl groups at 2- and 6-positions (Figure 1), showed narrow absorption and emission peaks with a 1−4 nm red shift compared to the dye **1**. From Table 1, it can be seen that a change in solvent polarity had little influence on shapes and positions of absorption and emission bands. The dye **3** compared to the dye **2** in different organic solvents show sharper absorption and emission bands with slightly lower fluorescence quantum yields (ranging from 0.71 to 0.89) (Table 1). Table 1 reveals the decrease in fluorescence lifetimes of the dye **3** in different solvents compared to the dyes **1** and **2**.

The dye **4**, in which there are benzyl groups at 2- and 6-positions and no substituent at the *meso* positon (Figure 1), shows sharper absorption and emission bands compared to those of the dyes **1** and **2** with a red shift of 7−9 and 2−3 nm in absorption and emission, respectively, relative to that of the dye **1**, resulting in the decrease in Stokes shift. The dye **4** shows good fluorescence quantum yields ranging from 0.74 to 0.96 in different solvents and has a comparable fluorescence lifetime with that of the dye **1** (Table 1). We have observed a considerable enhancement in the molar extinction coefficients (ε_{max}) at absorption maxima of the novel PM dyes **2**−**4** (Table 1) in solvents of different polarities.

Laser Characteristics. Interestingly, compared to ethanol, we observed surprisingly high photostability of the well-known laser dye **1** (Table 2) in 1,4-dioxane. Therefore, 1,4-dioxane solutions of the dye **1** and also that of the dyes **2**−**4** were comparatively evaluated for laser performances using frequency doubled (532 nm) output of a pulsed Nd:YAG laser as an excitation source. The results of the dye concentration-dependent broad-band lasing studies of 1,4-dioxane solutions of the PM dyes **1**−**4** are presented in Table 2 and shown in Figures 4 and 5. The lasing efficiency values of the dyes **1**−**4** in 1,4-dioxane (Figure 4) followed the expected pattern that is initially increasing with dye concentration, reaching a maximum value, followed by a decrease at higher concentration. The maximum broad-band lasing efficiency values (η) of the dyes **1**−**4** at their respective optimum dye concentrations are shown in Figure 5 and are also listed in Table 2. Lasing efficiency of the dyes **1**−**4** followed the similar pattern as that observed for their respective fluorescence quantum yields (Φ_{fl}) and molar extinction coefficient (ε_{max}) values. This suggests that incorporation of benzyl groups at 2- and 6-positions, similar to photophysical properties, had no or very little effect on respective lasing profiles of the dyes **2**−**4**. For each dye (**1**−**4**) laser, the spatial profile of lasing output was almost circular at the respective maximum lasing efficiency values.[12d] From Table 2, it can be seen that the dye **1** shows almost the same lasing efficiency in 1,4-dioxane compared to that in ethanol, but the concentration required to obtain the maximum lasing efficiency in 1,4-dioxane (0.92 mM) is slightly higher than that that in ethanol (0.83 mM). However, interestingly, the dyes **2** (0.35 mM) and **4** (0.59 mM) showed similar maximum lasing efficiency in 1,4-dioxane using a much lower concentration as that of the dye **1** (0.83 mM).

As expected, the dye **3** (0.51 mM) showed a slightly lower maximum lasing efficiency (38.2%) compared to that of dyes **1**, **2**, and **4**, which can be attributed to free rotation of the phenyl group at the *meso* position, leading to the increased loss of excitation energy by a nonradiative decay process (Table 1). The dyes **2**−**4** in 1,4-dioxane produce the maximum lasing

Scheme 3. Synthesis of the Dye 4

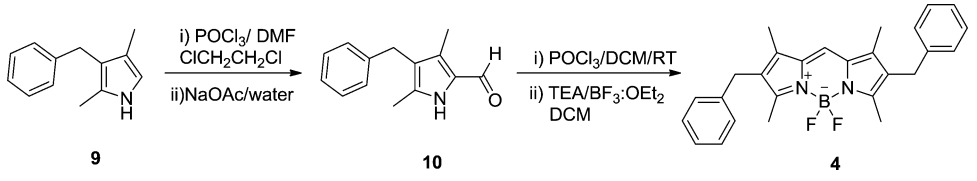

DOI: 10.1021/acs.joc.5b00654
J. Org. Chem. 2015, 80, 6152−6164

Table 1. Photophysical Parameters of the Dyes 1−4 in Various Solvents

solvent	λ_{abs}[a] (nm)	fwhm[b] (nm)	fwhm[b] (cm^{-1})	λ_{em}[c] (nm)	fwhm[d] (nm)	fwhm[d] (cm^{-1}))	$\Delta\nu$[e] (nm)	$\Delta\nu$[e] (cm^{-1})	$\varepsilon_{max}/10^{4}$[f] (M^{-1} cm^{-1})	Φ_{fl}[g]	τ[h] (ns)	$k_r/10^{8}$[i] (s^{-1})	$k_{nr}/10^{8}$[j] (s^{-1})
								dye **1**					
EtOH	518	25.3	957.2	533	41.5	1425.2	15	543.3	8.1	0.84[k]	6.19	1.36	0.258
1,4-dioxane	519	25.0	941.8	533	40.9	1399.8	14	506.1	8.4	0.83[k]	5.48	1.52	0.310
n-heptane	523	21.5	802.3	534	40.4	1381.1	11	393.9	9.1	0.98	6.03	1.63	0.033
								dye **2**					
ACN	514	26.3	1006.3	536	39.7	1381.4	22	799	13.4	0.82	n.d.	n.d.	n.d.
DMF	517	26.7	1009.7	539	37.2	1288.3	22	789	12.2	0.88	n.d.	n.d.	n.d.
DMSO	518	27.2	1027.4	540	42.5	1455.7	22	787	13.0	0.89	n.d.	n.d.	n.d.
MeOH	516	25.8	981.6	536	40.2	1396.9	20	723	11.2	0.78	n.d.	n.d.	n.d.
EtOH	517	26.3	996.8	536	39.7	1369.0	19	686	11.7	0.80	5.39	1.48	0.371
acetone	516	25.5	972.1	536	41.0	1419.5	20	723	13.8	0.86	n.d.	n.d.	n.d.
EtOAc	516	25.4	966.9	536	40.1	1385.9	20	723	10.2	0.86	n.d.	n.d.	n.d.
$CHCl_3$	521	24.5	913.4	537	36.7	1350.9	16	572	10.1	0.80	n.d.	n.d.	n.d.
1,4-dioxane	518	25.0	941.6	535	39.7	1365.3	17	613	11.6	0.87	4.88	1.78	0.266
n-heptane	520	22.0	821.1	536	38.3	1313.4	16	574	10.5	0.97	6.01	1.61	0.049
								dye **3**					
ACN	520	24.3	905.9	534	26.4	922.9	14	504	12.8	0.71	n.d.	n.d.	n.d.
DMF	523	24.1	886.1	537	26.7	923.4	14	498	12.1	0.74	n.d.	n.d.	n.d.
DMSO	524	24.3	893.3	538	26.9	924.6	14	497	12.2	0.89	n.d.	n.d.	n.d.
MeOH	521	23.6	878.0	535	26.1	812.1	14	502	11.6	0.81	n.d.	n.d.	n.d.
EtOH	522	23.7	877.1	535	26.0	907.9	13	465	11.4	0.74	4.73	1.56	0.549
acetone	521	23.1	857.3	535	25.1	874.4	14	502	12.7	0.74	n.d.	n.d.	n.d.
EtOAc	521	23.0	851.4	535	25.4	887.5	14	502	11.6	0.79	n.d.	n.d.	n.d.
$CHCl_3$	525	22.9	838.7	536	26.2	901.2	11	391	12.5	0.77	n.d.	n.d.	n.d.
1,4-dioxane	523	22.8	839.5	537	25.8	893.0	14	498	12.2	0.80	4.17	1.92	0.479
n-heptane	523	21.5	791.8	537	24.7	859.9	14	498	10.6	0.87	4.42	1.97	0.294
								dye **4**					
ACN	524	27.9	1037.5	537	21.9	764.3	13	462	10.0	0.74	n.d.	n.d.	n.d.
DMF	526	28.0	1030.0	540	24.0	828.1	14	493	9.6	0.86	n.d.	n.d.	n.d.
DMSO	527	28.3	1037.9	541	24.0	825.4	14	491	10.0	0.89	n.d.	n.d.	n.d.
MeOH	526	27.1	999.8	538	21.5	749.6	12	424	10.5	0.79	n.d.	n.d.	n.d.
EtOH	527	27.5	1012.5	536	23.6	814.9	9	319	9.7	0.83	6.0	1.38	0.283
acetone	525	26.7	987.1	538	22.7	789.0	13	460	11.3	0.84	n.d.	n.d.	n.d.
EtOAc	526	26.0	970.0	535	23.1	799.0	9	320	11.0	0.85	n.d.	n.d.	n.d.
$CHCl_3$	532	23.5	845.1	540	22.6	769.6	8	279	12.1	0.85	n.d.	n.d.	n.d.
1,4-dioxane	528	25.6	936.1	537	23.1	794.8	9	317	11.4	0.86	5.8	1.48	0.241
n-heptane	530	17.8	639.0	536	19.7	680.6	6	211	9.9	0.96	n.d.	n.d.	n.d.

[a]Wavelength at absorption maximum. [b]fwhm of longest wavelength absorption spectral band. [c]Wavelength at emission maximum. [d]fwhm of emission spectral band. [e]Stokes shift. [f]Molar extinction coefficient at absorption maximum. [g]Fluorescence quantum yield calculated using PM567 in ethanol (Φ_{fl} = 0.84) as standard. [h]Fluorescence lifetime. [i]Radiative rate constant. [j]Nonradiative rate constant. [k]Values taken from ref 10b. n.d. = not determined.

DOI: 10.1021/acs.joc.5b00654
J. Org. Chem. 2015, 80, 6152−6164

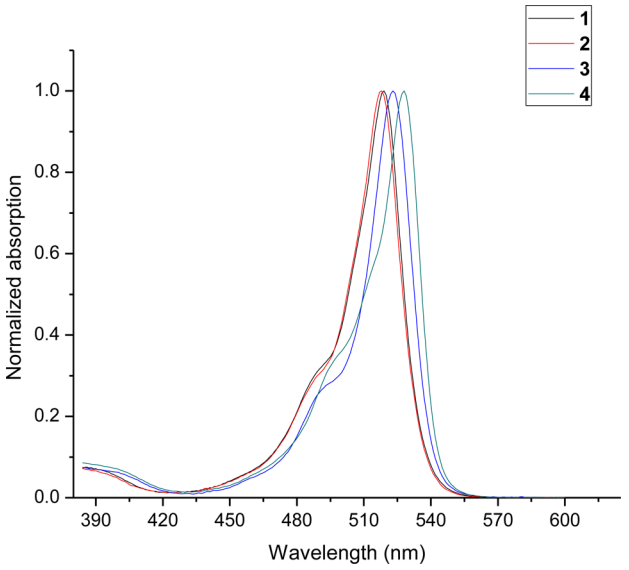

Figure 2. Normalized absorption spectra of the dyes **1**–**4** in 1,4-dioxane.

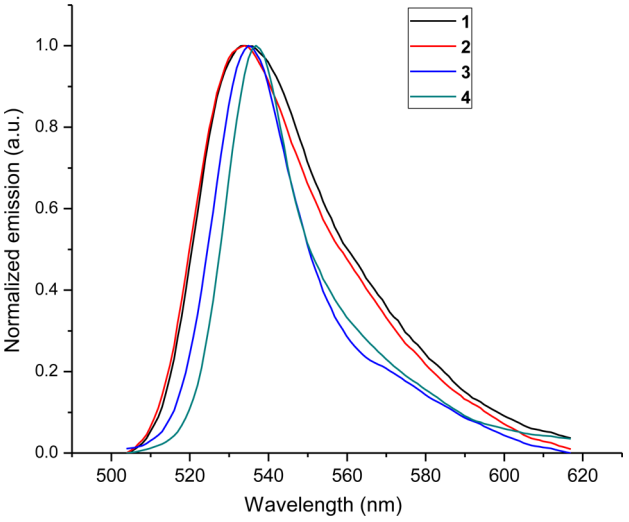

Figure 3. Normalized emission spectra of the dyes **1**–**4** in 1,4-dioxane. Excitation wavelength was 490 nm.

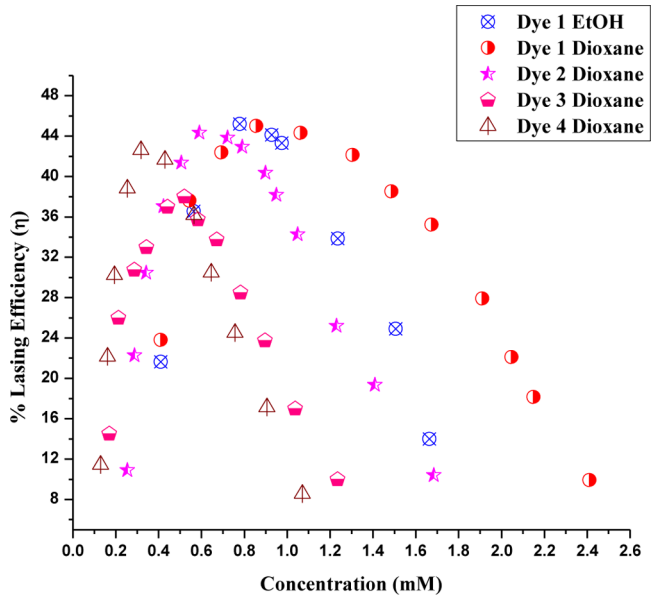

Figure 4. Concentration-dependent broad-band lasing efficiency of the PM dyes **1**–**4** in 1,4-dioxane, determined by 532 nm irradiation with a Q-switched Nd:YAG laser.

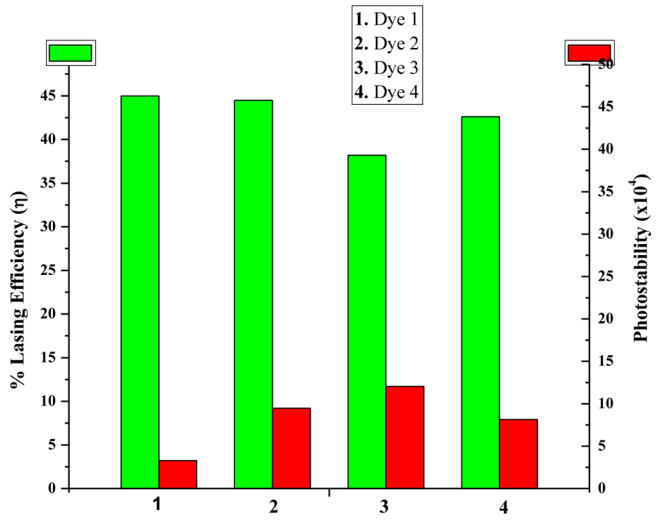

Figure 5. Broad-band lasing efficiencies (% η) and photostabilities (Φ_{pd}^{-1}) of the BODIPY dyes **1**–**4** in 1,4-dioxane, determined by pumping with 532 nm radiation of a Q-switched (10 Hz) Nd:YAG laser.

efficiency at relatively lower concentrations as that of the dye **1**. Beneficially, it would reduce the losses due to the ground state absorption (GSA) at high power dye amplifier operations, improving their laser performances.[12d] The dyes **2** and **4** have almost the same ε_{max} (Table 1), but the required concentration to obtain the maximum lasing efficiency in the case of the dye **4** is far less than that of the dye **2**, which can be attributed to the red-shifted absorption maxima of the dye **4** (528 nm),

Table 2. Lasing Characteristics of the PM Dyes 1–4[a] in 1,4-Dioxane

dye	conc.[b] (mM)	η[c] (%)	Φ_{pd}^{-1}[e]	Φ_{pd}^{-1} of **1** in dioxane/Φ_{pd}^{-1} of **1** in EtOH	Φ_{pd}^{-1} of **2**–**4** in dioxane/Φ_{pd}^{-1} of **1** in dioxane
1	0.83	45.2[d]	1.7×10^3[f]	18.82	
	0.92	45.0	3.2×10^4		
2	0.59	44.5	9.2×10^4		2.88
3	0.51	38.2	11.7×10^4		3.66
4	0.35	42.6	7.9×10^4		2.47

[a]Different concentrations of the dyes were used to maintain the optical density (O. D.) values of their solution at ~2.5 (1 mm cell) at 532 nm for photostability (Φ_{pd}^{-1}) determination (error: ± 1%). [b]Concentration of the dye required to obtain maximum lasing efficiency. [c]Broad-band lasing efficiency in 1,4-dioxane (error: ± 1%). [d]Broad-band lasing efficiency of the dye **1** in ethanol (error: ± 1%). [e]Photostability in 1,4-dioxane (error: ± 1%). [f]Photostability of the dye **1** in ethanol taken from our earlier work.[9]

DOI: 10.1021/acs.joc.5b00654
J. Org. Chem. 2015, 80, 6152–6164

appearing closer to the pump beam wavelength at 532 nm compared to that of the dye **2** (518 nm).

Photostability Characteristics. The quantum yield of photodegradation (Φ_{pd}) or photostabilities (Φ_{pd}^{-1}) of the dyes **1**−**4** in air-equilibrated 1,4-dioxane solutions were measured under nonlasing conditions and are enlisted in Table 2, column 4, and are also shown in Figure 5. The enhancement in Φ_{pd}^{-1} value of the dye **1** in 1,4-dioxane compared to that in ethanol is shown in column 5, and the enhancement in Φ_{pd}^{-1} of the dyes **2**−**4** in 1,4-dioxane compared to that of the dye **1** in 1,4-dioxane is shown in column 6 of Table 2. The reason for selecting 1,4-dioxane solvent for detail laser study is that the PM dyes **2**−**4** as well as dye **1** showed a large enhancement in photostability in 1,4-dioxane than that in commonly used ethanol.

Among the dyes **2**−**4**, the dye **3** has the highest photostability, followed by the dye **2** and then **3**. In 1,4-dioxane, the dyes **2**−**4** are found to be more photostable by 2.88, 3.66, and 2.47 times, respectively, than that of dye **1** (Table 2). The photostability results revealed that the benzyl groups at 2- and 6-positions, even though not in conjugation with the PM core, induced a positive effect on photostability. The negative inductive effect (−I) of the benzyl groups may be responsible to reduce the electron density on the PM core to some extent.

Cyclic Voltammetry. Cyclic voltammetry analysis of the BODIPY dyes **1**−**4** showed a reversible peak in each case in the anodic portion of the cyclic voltammograms (Figure 6), which

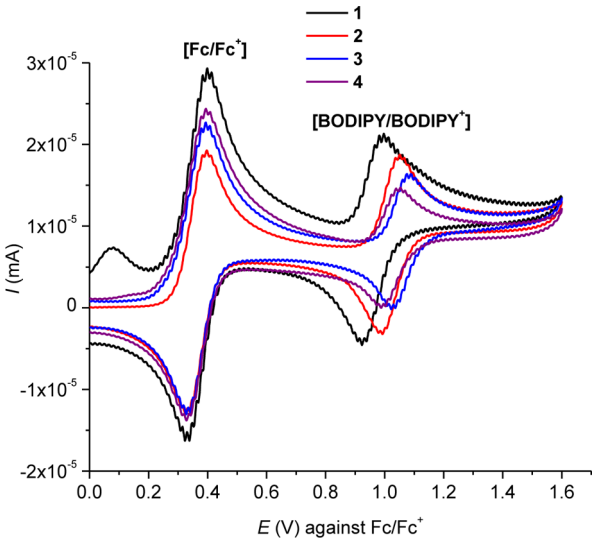

Figure 6. Cyclic voltammograms of the BODIPY dyes **1**−**4** in acetonitrile at room temperature.

was assigned to one-electron oxidation of the BODIPY unit.[19] From Figure 6, it can be seen that the incorporation of the benzyl groups at 2- and 6-positions of the PM chromophore has a positive effect on the oxidation potentials (E_{ox}). The dyes **2** (E_{ox}^{0} = 1.054 V), **3** (E_{ox}^{0} = 1.083 V), and **4** (E_{ox}^{0} = 1.047 V) possess higher oxidation potentials as compared to that of the dye **1** (E_{ox}^{0} = 0.997 V), by 57, 86, and 50 mV, respectively. The above CV data suggested that the trend in probability of oxidation of the dyes increases in the order **3** < **2** < **4** < **1**, which agrees well with the trend in observed laser photostabilities of the dyes (**1** < **4** < **2** < **3**). To obtain further insight on the structure−property relationship of these dye molecules, we have carried out DFT and TD-DFT calculations, which are discussed in the next sections.

THEORETICAL INTERPRETATIONS

The BODIPY dyes **1**−**4** possess a compact chromophore with high molar extinction coefficients, which can be used to explore the electronic structure of BODIPY chromophores in various solvents by means of DFT and TD-DFT calculations using the B3LYP/6-31G(d) level of theory. In our studies, we have analyzed the absorption and emission characteristics of the PM dyes **1**−**4** and correlated them with the photophysical and photostability properties.

Geometrical Parameters. The dyes **1**−**4** were optimized in their S_0 and S_1 states with the help of DFT and TD-DFT using the B3LYP/6-31G(d) functional for all the atoms in vacuum and various organic solvents, but results obtained in 1,4-dioxane are presented in Table 3. The BODIPY unit was found to be perfectly planar in ground state optimized geometries of dyes **1**−**4** with very little or negligible displacement (0.6−1.1°) of the boron atom, which revealed an effective overlap of *p*-orbitals. In the dye **3**, the *meso* (C-8) phenyl substituent oriented orthogonally with the BODIPY plane with a little twist making an angle of 92.3° in the S_0 state, suggesting no electronic interactions with the PM core.

The phenyl rings of 2- and 6-substituents in the case of the dyes **2**−**3** appear to make an angle of 35.2, 34.7, and 36.4°, respectively, in the S_0 state. Shortening of the C8−C9 bond by 0.01 Å is observed in the case of the dye **3**. A considerable decrease in the length of the bond between C10−C11 is observed upon changing groups at 2- and 6-positions of the PM core from ethyl (the dye **1**) to benzyl (the dyes **2**−**4**), from 1.540 Å for the dye **1** to 1.526, 1.527, and 1.527 Å for the dyes **2**−**4**, respectively, in the S_0 state.

The S_1 optimized states of the dyes **1**−**4** revealed that there is no remarkable change in the geometry from that of the respective S_0 states, except in the case of the dye **3**, where the boron atom was found to be displaced more from the PM core by 5.3° and the *meso* phenyl from its orthogonal arrangement displaced more by 16.1° (Table 3).

Mulliken Charges. The analysis of Mulliken charge distribution of the dyes **2**−**4** in solvent 1,4-dioxane (Table 4 and Figures S1−S4, Supporting Information), relative to that of the dye **1** over the atoms of the PM core (C-2, C-7′, C-8, C-9, and C-10), showed considerable change in the electron densities. Changing the C-8 methyl substituent to the phenyl (dye **3**) led to a little increase in the electron density at C-7, but an abrupt decrease in the electron density at C-8 is observed.

A similar trend is observed in the dye **4**, a hydrogen at the *meso* position, but the change in electron density at C-7′ and C-8 is more pronounced.

Also, when the ethyl substituents of the dye **1** at 2- and 6-positions were changed to benzyl groups in the dyes **2**−**4**, the abrupt decrease in the electron density at C-2 and C-10 is observed. From this, it is clear that, though the phenyl rings in benzyl groups are not in conjugation with the BODIPY chromophore, they still can alter the electronic properties of the PM moiety, leaving a positive impact on its photostability.

When the Mulliken charges in S_0 states of the dyes **1**−**4** were compared with their respective S_1 states, there is no or negligible change in the electron densities over the various atoms of the PM moiety (Table S1, Supporting Information), which is consistent with experimental observations of small Stokes shift of the PM dyes.

DOI: 10.1021/acs.joc.5b00654
J. Org. Chem. 2015, 80, 6152−6164

Table 3. Selected Bond Lengths, Bond Angles, and Torsional Angles of the Dyes 1−4, Optimized in 1,4-Dioxane Media Using B3LYP/6-31G(d) Level of Theory

atom no.	dye 1		dye 2		dye 3		dye 4	
	GS[a]	ES[b]	GS	ES	GS	ES	GS	ES
				bond lengths (Å)				
C1−C2	1.399	1.412	1.399	1.408	1.400	1.408	1.400	1.401
C2−C3	1.417	1.415	1.418	1.425	1.416	1.425	1.419	1.425
C3−N3′	1.348	1.350	1.345	1.350	1.349	1.349	1.352	1.350
N3′−B4	1.552	1.543	1.554	1.544	1.553	1.543	1.562	1.554
B4−F4′	1.397	1.403	1.396	1.402	1.397	1.402	1.395	1.401
C7′−C8	1.409	1.424	1.411	1.428	1.404	1.429	1.389	1.392
C8−C9	1.509	1.505	1.509	1.505	1.496	1.486		
C6−C10	1.506	1.499	1.507	1.502	1.507	1.502	1.506	1.503
C10−C11	1.540	1.545	1.526	1.526	1.527	1.527	1.526	1.526
				bond angles (deg)				
C3−N3′−B4	125.2	124.9	125.1	124.9	125.4	124.3	126.8	125.6
N3′−B4−F4′	109.8	109.9	109.9	109.9	109.7	110.3	109.7	110.1
F4′−B4−F4″	109.9	109.1	110.1	109.2	110.1	109.2	110.3	109.3
				dihedral angles (deg)				
C2−C3−N3′−B4	179.4	179.9	178.7	178.5	179.8	174.5	179.7	179.8
C7′−C8−C9−C12					92.3	108.4		
C6−C10−C11−C11′			35.2	42.4	34.7	40.9	36.4	42.1

[a]Computed geometrical parameters of molecules in ground state. [b]Computed geometrical parameters of molecules in excited state.

Table 4. Mulliken Charges (e.s.u.) on Different Selected Atoms of the Dyes 1−4 at Their Respective Optimized Ground State Geometries, Calculated by B3LYP/6-31G(d) Level of Theory in 1,4-Dioxane

dye	C-1	C-2	C-3	N-3′	B-4	C-7′	C-8	C-9	C-10
1	0.087	0.020	0.315	−0.576	0.693	0.182	0.116	−0.013	−0.055
2	0.087	0.011	0.327	−0.578	0.693	0.182	0.118	−0.010	−0.124
3	0.088	0.008	0.333	−0.582	0.695	0.215	−0.027	0.023	−0.122
4	0.088	0.005	0.329	−0.586	0.697	0.248	−0.056		−0.120

Table 5. Calculated Absorption Parameters of the PM Dyes 1−4 in Ethanol, 1,4-Dioxane, and *n*-Heptane Using TD-DFT (B3LYP/6-31G(d)) Method

dye	ethanol			1,4-dioxane			*n*-heptane		
	$E_{S0\rightarrow S1}$[a] (eV)	λ_{ab}[b] (nm)	f[c]	$E_{S0\rightarrow S1}$ (eV)	λ_{ab} (nm)	f	$E_{S0\rightarrow S1}$ (eV)	λ_{ab} (nm)	f
1	2.8247	438.9	0.5933	2.7524	450.5	0.5823	2.8100	441.2	0.6202
2	2.8133	440.7	0.7023	2.7950	443.6	0.7384	2.8002	442.8	0.7331
3	2.7882	444.7	0.6881	2.7778	446.3	0.7257	2.7832	445.5	0.7195
4	2.8088	441.4	0.7036	2.7968	443.3	0.7462	2.8026	442.4	0.7399

[a]Energy required for the $S_0 \rightarrow S_1$transition. [b]Calculated maximum absorption wavelength. [c]Oscillator strength.

Calculated Absorptions and Emissions. The ground state optimized structures of dyes in solvents of various polarities were subjected to TD first 20 states calculations[20] in order to get vertical excitations using the B3LYP/6-31G(d) method. This led to more understanding of the absorption properties of the synthesized PM dyes, and the results are summarized in Tables 5 and 6.

The results of DFT and TD-DFT also suggest no or negligible influence of the change in solvent polarity on the absorption of the PM dyes (Table 6). The absorption maxima in all different solvents are centered around 440−447 nm with 14.5−16.2% deviations from the experimental values of absorption maximum. In all the solvents for the dyes **2**−**4**, the vertical excitations are associated with the HOMO → LUMO transitions and strong oscillator strengths ranging from 0.68 to 0.74. For comparison, we have also performed the same calculations for the dye **1** (Table 5) in selected solvents and got similar observations like the dyes **2**−**3**.

From the increased oscillator strengths of the dyes **2**−**4** in various solvents compared to that of the dye **1** (Table 5), it can be seen that TD-DFT also accounts for the enhanced molar extinction coefficients of the dyes **2**−**4**.

The minimum energy S_1, B3LYP/6-31G(d), optimized structures were further subjected to the TD 10 states energy calculations[20] in order to get emissions, and the results are summarized in Table 6. From the calculated emissions, it can be seen that, like vertical excitations, there is negligible influence of changes in solvent polarity on the emission of novel PM dyes **2**−**4**. The TD-DFT emission maxima calculated for the dye **2** in various solvents are associated with the LUMO → HOMO transition and centered around 462.8−471.0 nm with an oscillator strength of the order of 0.59−0.64 (Table 6). Similarly, the TD-DFT emissions for the dye **3** in various solvents are associated with the LUMO → HOMO transition and centered around 463.5−474.3 nm with oscillator strengths in the range of 0.59−0.60 (Table 6).

DOI: 10.1021/acs.joc.5b00654
J. Org. Chem. 2015, 80, 6152−6164

Table 6. TD-DFT Absorption and Emission Parameters of the Dyes 2−4 in Various Solvents

		TD-B3LYP/6-31G(d) absorptions					TD-B3LYP/6-31G(d) emissions			
solvent	λ_{abs}[a] (nm)	λ_{abs}[b] (nm)	f[c]	D[d] (%)	major contribution[e]	λ_{em}[f] (nm)	λ_{em}[g] (nm)	f[h]	D[i] (%)	major contribution
					dye **2**					
ACN	514	440.2	0.6970	14.4	H→L(94.77)	536	536.0	0.6258	13.8	L→H(94.99)
DMF	517	442.6	0.7163	14.4	H→L(95.31)	539	539.0	0.6436	13.8	L→H(95.49)
DMSO	518	442.2	0.7129	14.6	H→L(95.26)	540	540.0	0.6412	14.0	L→H(95.43)
MeOH	516	439.7	0.6935	14.8	H→L(94.67)	536	536.0	0.6222	13.8	L→H(94.89)
EtOH	517	440.7	0.7023	14.8	H→L(94.92)	536	536.0	0.6289	13.6	L→H(95.08)
acetone	516	440.7	0.7026	14.6	H→L(94.91)	536	536.0	0.6281	13.6	L→H(95.06)
EtOAc	516	441.4	0.7149	14.5	H→L(95.20)	536	536.0	0.6236	13.2	L→H(94.92)
$CHCl_3$	521	443.6	0.7332	14.9	H→L(96.64)	537	537.0	0.6353	12.9	L→H(95.25)
1,4-dioxane	518	443.6	0.7384	14.4	H→L(95.76)	535	535.0	0.6097	12.0	L→H(94.45)
heptane	520	442.8	0.7331	14.9	H→L(95.62)	536	536.0	0.5931	12.1	L→H(93.91)
					dye **3**					
ACN	520	444.2	0.6827	14.6	H→L(93.75)	534	463.6	0.5995	13.2	L→H(93.47)
DMF	523	446.6	0.7033	14.6	H→L(94.41)	537	466.0	0.6187	13.2	L→H(94.11)
DMSO	524	446.5	0.6985	14.8	H→L(94.29)	538	465.5	0.6165	13.5	L→H(94.03)
MeOH	521	443.7	0.6789	14.8	H→L(93.63)	535	463.2	0.5955	13.4	L→H(93.34)
EtOH	522	444.7	0.6881	14.8	H→L(93.92)	535	464.3	0.6022	13.2	L→H(93.58)
acetone	521	444.6	0.6882	14.7	H→L(93.92)	535	464.4	0.6007	13.2	L→H(93.54)
EtOAc	521	444.7	0.7028	14.7	H→L(94.31)	535	466.9	0.5913	12.7	L→H(93.35)
$CHCl_3$	525	447.1	0.7197	14.8	H→L(94.83)	536	469.6	0.6031	12.4	L→H(93.78)
1,4-dioxane	523	446.3	0.7257	14.7	H→L(94.91)	537	473.5	0.5659	11.8	L→H(92.66)
heptane	523	445.5	0.7195	14.8	H→L(94.71)	537	474.2	0.5440	11.7	L→H(91.85)
					dye **4**					
ACN	524	440.9	0.6975	15.9	H→L(91.73)	537	460.4	0.6274	14.3	L→H(92.52)
DMF	526	443.3	0.7206	15.7	H→L(92.58)	540	462.9	0.6479	14.3	L→H(93.27)
DMSO	527	443.0	0.7167	15.9	H→L(92.44)	541	462.4	0.6457	14.5	L→H(93.18)
MeOH	526	440.5	0.6932	16.3	H→L(91.57)	538	460.0	0.6233	14.5	L→H(92.36)
EtOH	527	441.4	0.7036	16.2	H→L(91.44)	536	461.5	0.6620	13.9	L→H(93.98)
acetone	525	441.3	0.7041	15.9	H→L(91.95)	538	461.1	0.6316	14.3	L→H(92.59)
EtOAc	526	441.6	0.7183	16.0	H→L(92.34)	535	463.5	0.6185	13.4	L→H(92.22)
$CHCl_3$	532	442.7	0.7402	16.8	H→L(93.08)	540	466.5	0.6282	13.6	L→H (92.60)
1,4-dioxane	528	443.3	0.7462	16.0	H→L(93.16)	537	473.4	0.5450	11.8	L→H(89.68)
heptane	530	442.4	0.7399	16.5	H→L(92.92)	536	479.0	0.4697	10.6	L→H(86.53)

[a]Experimental maximum absorption wavelength. [b]TD-B3LYP/6-31G(d) absorption. [c]Oscillator strength of vertical excitation. [d]Deviation from the observed absorption maximum. [e]Major electronic transition. [f]Experimental maximum emisson wavelength. [g]TD-B3LYP/6-31G(d) emission. [h]Oscillator strength of vertical emission. [i]Deviation from the observed emission maximum; H = HOMO; L = LUMO.

Table 7. Dipole Moments of the PM Dyes 1−4 in Various Solvents Using TD-DFT (B3LYP/6-31G(d)) Method

	dye **1**		dye **2**		dye **3**		dye **4**	
solvent	μ_0[a] (D)	μ_1[b] (D)	μ_0 (D)	μ_1 (D)	μ_0 (D)	μ_1 (D)	μ_0 (D)	μ_1 (D)
DMSO	n.d.	n.d.	5.8223	5.9851	5.9592	6.1635	5.1088	5.1860
DMF	n.d.	n.d.	5.8014	5.9649	5.9440	6.1472	5.0902	5.1675
ACN	n.d.	n.d.	5.7971	5.9607	5.9406	6.1439	5.0863	5.1636
MeOH	n.d.	n.d.	5.7872	5.9511	5.9334	6.1362	5.0775	5.1494
EtOH	5.7137	5.8945	5.7517	5.9167	5.9058	6.1084	5.0461	5.0801
acetone	n.d.	n.d.	5.7207	5.8866	5.8815	6.0840	5.0201	5.0839
EtOAc	n.d.	n.d.	5.3401	5.5127	5.5755	5.7833	4.6761	4.7620
CHCl3	n.d.	n.d.	5.2149	5.3924	5.4730	5.6908	4.5655	4.6589
dioxane	4.6850	4.8960	4.6871	4.8876	5.0186	5.2572	4.1036	4.2771
heptane	4.5632	4.7791	4.5640	4.7738	4.9075	5.1566	3.9966	4.2431

[a]Dipole moment in ground state (S_0). [b]Dipole moment in excited state (S_1); n.d. = not determined.

Dipole Moments. The TD-DFT calculated dipole moments of the dyes **1**−**4** in solvents of different polarities are summarized in Table 7. The calculations revealed a minimum change in dipole moments of the S_0 and S_1 states of the dyes **1**−**4** in the solvents of various polarities, supporting the weak solvatochromism. The calculated dipole moments of the dyes **2**−**3**, both in the ground (μ_0) and the excited singlet (μ_1) states, were higher compared to that of the dye **1**, suggesting better polarizability of the dyes **2** and **3**.

However, as there is no substituent at the *meso* position in the case of the dye **4**, the dipole moments of the dye **4** in S_0 and S_1 are less compared to those of the dye **1**, suggesting poor

DOI: 10.1021/acs.joc.5b00654
J. Org. Chem. 2015, 80, 6152−6164

Table 8. Energy of HOMO, LUMO, and Band Gaps of the PM Dyes 1−4 in Ethanol, 1,4-Dioxane, and *n*-Heptane Using TD-DFT (B3LYP/6-31G(d)) Method

	ethanol			1,4-dioxane			*n*-heptane		
dye	E_H[a] (eV)	E_L[b] (eV)	$E_H - E_L$ (eV)	E_H (eV)	E_L (eV)	$E_H - E_L$ (eV)	E_H (eV)	E_L (eV)	$E_H - E_L$ (eV)
1	−5.361	−2.362	2.999	−5.246	−2.269	2.977	−5.235	−2.261	2.974
2	−5.432	−2.429	3.003	−5.334	−2.349	2.984	−5.324	−2.342	2.982
3	−5.456	−2.510	2.946	−5.332	−2.395	2.937	−5.319	−2.383	2.936
4	−5.469	−2.503	2.965	−5.374	−2.420	2.954	−5.365	−2.412	2.953

[a]Energy of highest occupied molecular orbital (HOMO). [b]Energy of lowest unoccupied molecular orbital (LUMO).

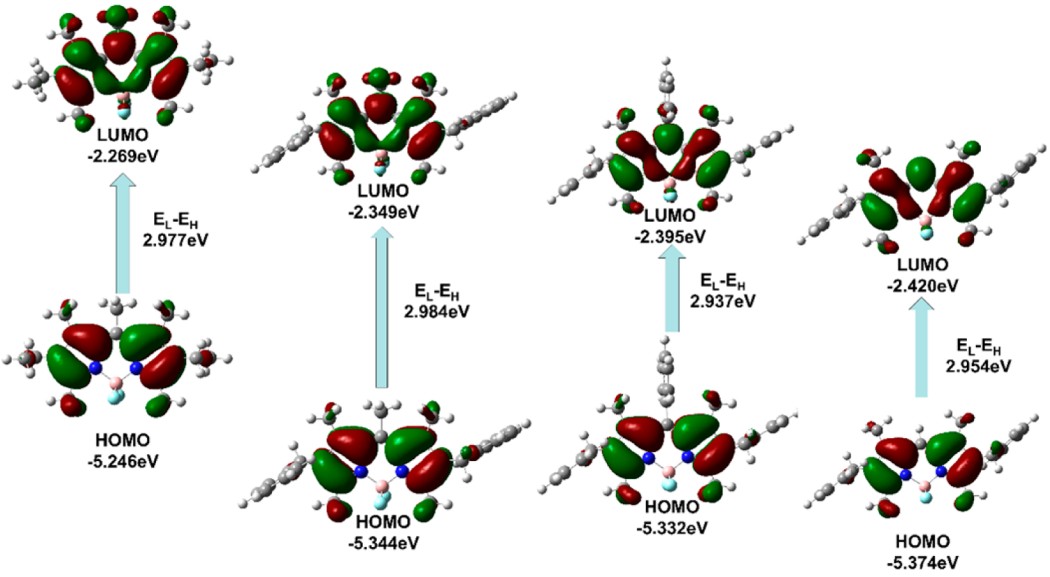

Figure 7. Frontier molecular orbitals of dyes **1**−**4** in 1,4-dioxane, calculated by the B3LYP/6-31G(d) level of theory (the orbital diagrams are plotted with the contour value of 0.02 a.u.).

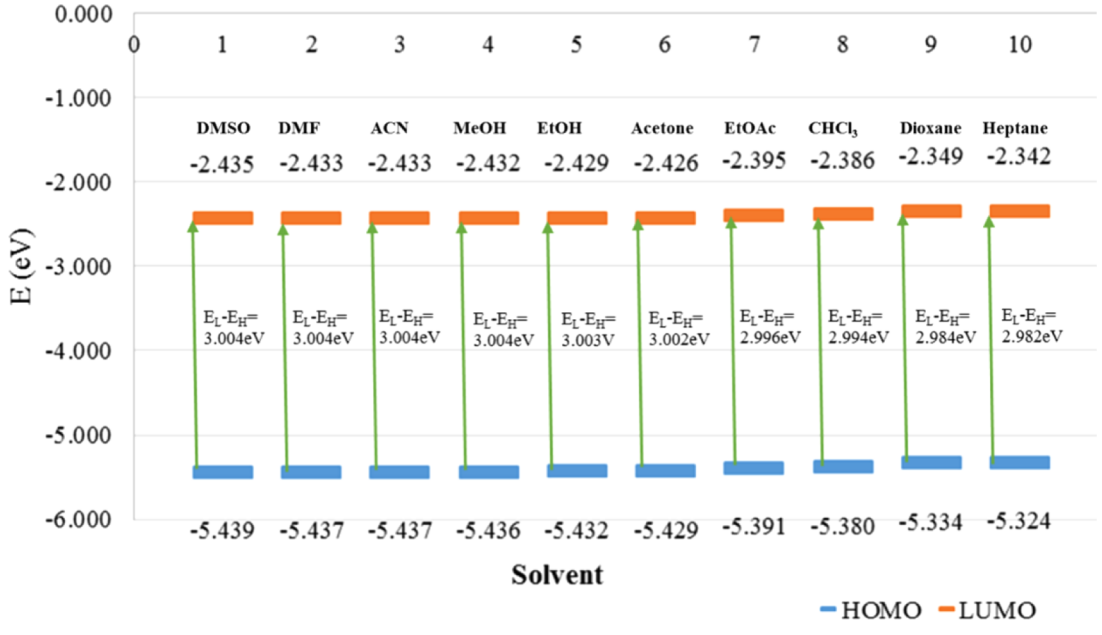

Figure 8. Energy gaps between HOMO and LUMO of the dye **2** in various solvents.

polarizability of the dye **4** relative to that of the dyes **1**−**3**. With the decrease in solvent polarity from DMSO to *n*-heptane, the dipole moments of the S_0 and S_1 states of the dyes **1**−**4** are found to be decreasing.

Molecular Orbital Energies. Energy levels of the frontier molecular orbitals, especially HOMO−1, HOMO, LUMO, and LUMO+1, and their spatial distributions can give the idea about behavior of the dye molecules in terms of photophysical properties, lasing properties, and photostabilities. The frontier

DOI: 10.1021/acs.joc.5b00654
J. Org. Chem. 2015, 80, 6152−6164

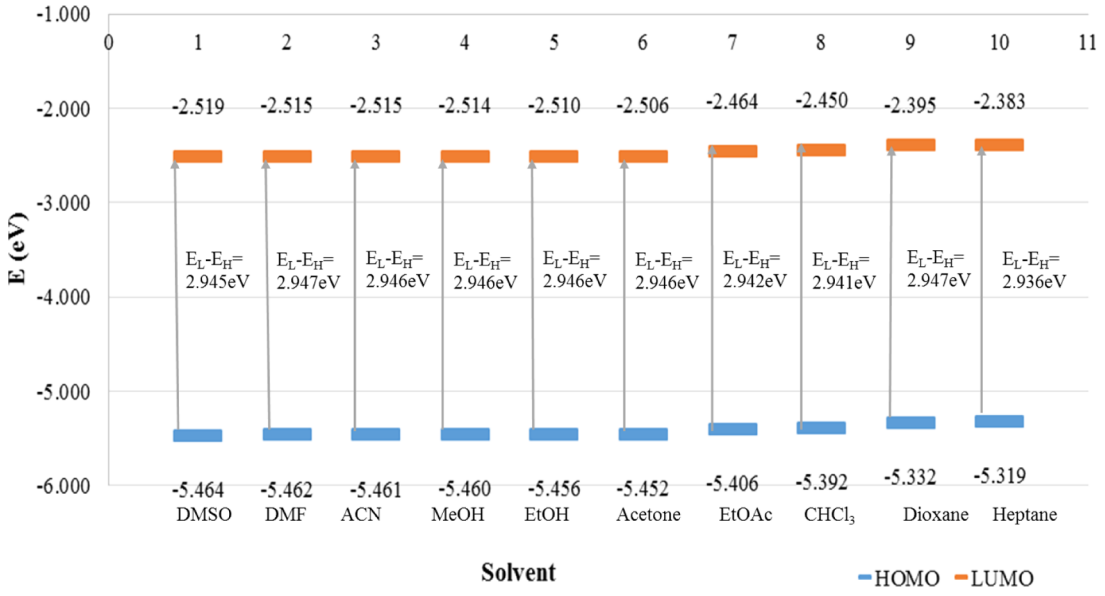

Figure 9. Energy gaps between HOMO and LUMO of the dye **3** in various solvents.

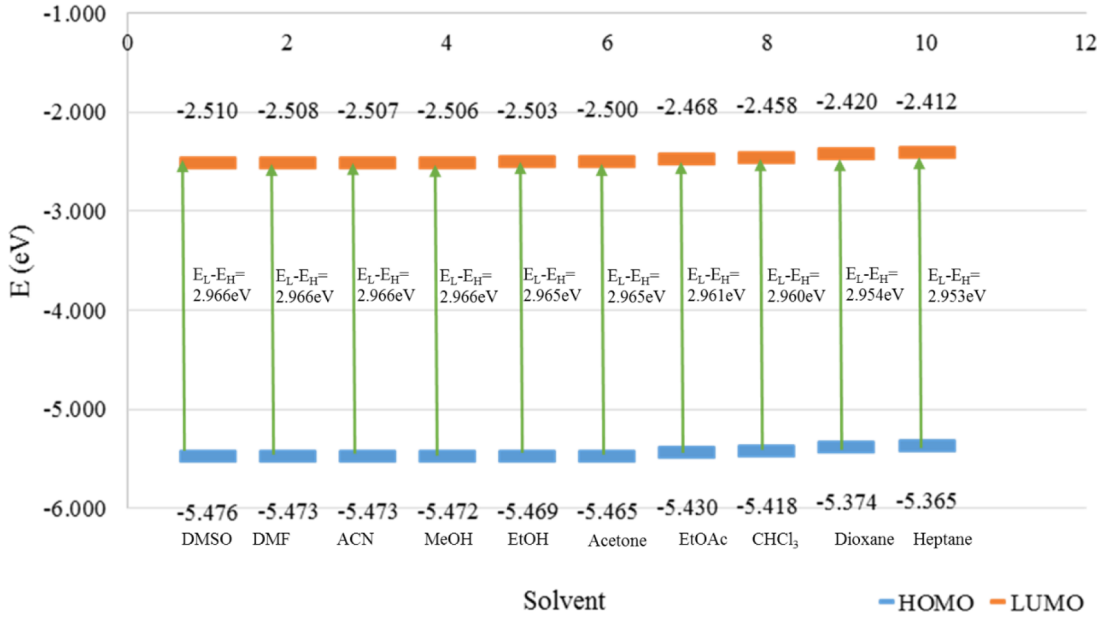

Figure 10. Energy gaps between HOMO and LUMO of the dye **4** in various solvents.

molecular orbitals of the dyes **1**−**4** in 1,4-dioxane, calculated by the B3LYP/6-31G(d) level of theory, are shown in Figure 7, and HOMO and LUMO energies and the band gaps of the dyes **1**−**4** in ethanol, 1,4-dioxane, and *n*-heptane and those of the dyes **2**−**4** in solvents of different polarities are summarized in Table 8 and Table S2 (Supporting Information), respectively, and are also shown in Figures 8−10.

From Figure 7, it can be seen that, in the HOMO of the dye **1**, the electron density is localized on the BODIPY core but completely away from N-3, N-3′, and B-4, but in the LUMO of the dye **1**, it can be seen that the electron density is distributed almost uniformly over the whole chromophore. From this, it is confirmed that the HOMO of the dye can easily react with the *in situ* generated singlet oxygen ($^1O_2$) upon laser excitation, because the C7′−C8 double bond has a maximum electron density in the HOMO compared to the LUMO (Figure 7).

In the case of the dyes **2**−**4**, the electron density in HOMO and LUMO shows similar observations like that of the dye **1**, confirming again the involvement of the HOMO of the dyes **2**−**4** in the photochemical reaction with single oxygen ($^1O_2$). Figures 8−10 and Table S2 (Supporting Information) reveal that, among the dyes **2**−**4**, the order of the band gap (HOMO → LUMO) is **2** > **4** > **3**, and for each of them, the band gap is found to be decreasing with the solvent polarity (dimethyl sulfoxide to *n*-heptane).

CONCLUSION

We have designed and synthesized three congeners of the widely used BODIPY laser dye PM567 by modifications at the 2- and 6-positions/or at both the 2- and 6-positions and the *meso* position. Remarkably, enhanced photostability and lower concentration of dye requirement to get comparable lasing

DOI: 10.1021/acs.joc.5b00654
J. Org. Chem. 2015, 80, 6152−6164

output in 1,4-dioxane relative to that of PM567 are the positive effects of the PM dyes, **2** and **4**. From superior laser properties and enhanced photostabilities relative to those of PM567, it may be envisaged that the dyes **2** and **4** can be used efficiently as laser dyes in the green-yellow region. The photophysical and laser properties of the synthesized PM dyes experimentally and structural, photophysical, and electronic properties by means of DFT and TD-DFT are extensively studied. These findings will be helpful for the future design and synthesis of efficient and photostable BODIPY laser dyes.

EXPERIMENTAL SECTION

General Methods. Laser grade Pyrromethene 567 was procured and used without any further purification. The purity of the dye was found to be >99%, as determined with spectroscopy and chromatographic methods. All the chemicals and spectroscopy grade solvents were obtained from the local suppliers unless otherwise mentioned and used as such without further purifications. All the common chemicals were of analytical grade. The solvents were purified by standard procedures. All the reactions were monitored by TLC (thin-layer chromatography) with detection by UV light. The FT-IR spectra were recorded on an FT/IR spectrometer. ^{1}H NMR, ^{13}C NMR, ^{11}B NMR, and ^{19}F NMR spectra were recorded on a 500 MHz instrument using TMS as an internal standard. HRMS analysis were done using a QTOF LC/MS spectrometer. Mass spectra were recorded on a mass spectrometer.

Photophysical Studies. The absorption spectra were recorded on a UV−vis spectrometer, and the corresponding maximum molar extinction coefficients (ε_{max}) were determined. The emission spectra were recorded on a fluorescence spectrophotometer using a 10 mm cuvette with a 2.5 nm slit width at a 490 nm excitation wavelength. The relative fluorescence quantum yields (Φ_{fl}) of the dyes **2**−**4** were determined using the dye **1** as a standard. The excited-state (S_1) lifetimes of the dyes **1**−**4** were determined by time-resolved fluorescence measurements carried out with an LED-based time-correlated single photon-counting (TCSPC) spectrometer. The fluorescence decays were measured with a 390 nm LED (1 MHz) excitation source and a TBX4 detection module coupled to a special PMT instrument. Following deconvolution analysis of the fluorescence decays, the time resolution of the present setup was around 50 ps. All the measurements were carried out at ambient temperature (298 ± 1 K), maintained with a microprocessor-based temperature controller.

Broad-Band Laser Study. The lasing studies of the dyes **1**−**4** in 1,4-dioxane were carried out by using a constructed broad-band dye laser setup (a dye cell of width ∼ 10 mm placed between a high reflectivity (∼100%) mirror and wedged output coupler (∼4% reflectivity)), transversely pumped by the second harmonic (at 532 nm) output of a Q-switched pulsed Nd:YAG laser at a repetition rate of 10 Hz with a pulse energy of around 4.2 mJ and fwhm of 5−7 ns. All the laser data for the dyes in 1,4-dioxane were measured by using the same dye laser setup, which is schematically shown in Figure S5 in the Supporting Information. The pump and the dye laser powers were measured with the same power meter. To determine the lasing efficiency at various concentrations of 1,4-dioxane solutions of the dyes **1**−**4**, initially the dye solution of higher concentration was tested in each case and then stepwise diluted. The absorbance of each dye solution was measured from which the dye concentration was calculated by using the formula, $A = \varepsilon bc$, where A is the absorbance, ε is the molar extinction coefficient at absorption maxima, b is the path length (0.1 cm), and c is the concentration.

Photostability Study. The quantum yield of the photodegradation (Φ_{pd}) of the dye is defined as the probability of the decomposition of the dye molecules by the absorbed pump photons. The photostability is expressed as the inverse of the Φ_{pd} value. A known quantity of the dye solution (2.5 mL) in a dye laser cuvette was exposed to a pump energy of 6.7−7.2 mJ at 532 nm. The concentration of the dye solution was chosen such that the pump beam was totally absorbed within the dye solution in the cuvette during the excitation of 3−4 h. The solution was constantly stirred with a Teflon-coated magnetic stirrer to avoid local heating. The number of photodegraded dye molecules in the exposed volume of the dye solutions was quantitatively estimated from the absorbance at the corresponding λ_{max} before and after photoexposure for a set period of time. The reflection loss of the pump beam on incident surfaces of the dye cell was determined by calculating the absorbed cumulative pump photons.

Electrochemical Studies. Cyclic voltammetry was performed at 25 °C in deoxygenated acetonitrile containing 0.1 M tetrabutylammonium hexafluorophosphate ($TBAPF_6$) and a solute concentration of 0.6−1 mM. The glassy carbon (2 mm diameter) was used as working electrode, platinum wire as counter electrode, and standard calomel electrode as reference electrode with ferrocene (∼1 mM) as an internal standard. The redox potentials were standardized with ferrocene (Fc) as the internal reference and referenced to SCE by taking E^0 (Fc/Fc^+) = +0.405 V versus SCE. All waves were monoelectronic.

Computational Details. All the computations were performed using the Gaussian 09 program package.[21] The ground state (S_0) geometry of the dyes was optimized using the DFT[22] method. The functional used was B3LYP (the B3LYP combines Becke's three-parameter exchange functional (B3)[23] with the nonlocal correlation functional by Lee, Yang, and Parr (LYP)).[24] The basis set used in both, DFT and TD-DFT methods for all the atoms was 6-31G(d). In order to verify whether the optimized structures have minimum energy, frequency computations were performed at the same level of theory. The vertical excitation energies and oscillator strengths were obtained for the 20 lowest $S_0 \rightarrow S_1$ transitions at the optimized ground state equilibrium geometries by using the time-dependent density functional theory (TD-DFT) using the same hybrid functional and basis set.[20,25a−g] To obtain their minimum energy geometries (which correspond to the emissive state), the low-lying first singlet excited states (S_1) of the dyes were relaxed using the TD-DFT. The emission wavelengths and oscillator strengths were obtained for the 10 lowest $S_1 \rightarrow S_0$ transitions at the optimized excited state equilibrium geometries by using TD-DFT using the same hybrid functional and basis set.[20] The frequency computations were also carried out at the same level of theory on the optimized geometry of the first excited state of the dyes. All the computations in the various solvents media were carried out using the self-consistent reaction field (SCRF) under the polarizable continuum model (PCM).[26a,b] The electronic absorption spectra, including wavelengths, oscillators strengths, and main configuration assignment, were systematically investigated using TD-DFT with the PCM model on the basis of the optimized ground structures.

Synthesis of 3-Benzylpentane-2,4-dione (6). To a stirred solution of acetyl acetone (5 g, 0.0499 mol) in acetone (25 mL) at 0 °C was added sodium carbonate (6.86 g, 0.0648 mol) in portions, and the mixture was allowed to stir for 15 min. Then, to this was added dropwise a solution of benzyl bromide (8.96 g, 0.0524 mol) in acetone (20 mL) for 15 min. The resulting mixture was allowed to stir at reflux temperature for 24 h. The cooled reaction mixture was filtered to remove solid sodium carbonate, the filtrate was concentrated under vacuum, and the pale yellow liquid obtained was allowed to stand for a 5−6 h. The off-white solid formed was discarded by decantation, and the obtained product (**6**), a pale yellow liquid, was used as such without any further purification for the next step. Crude yield: 8.37 g (88%).

Synthesis of Ethyl 4-Benzyl-3,5-dimethyl-1*H*-pyrrole-2-carboxylate (7). To a solution of ethyl acetoacetate (3.42 g, 0.0263 mol) in acetic acid (12 mL) at 0 °C was added a cold solution of sodium nitrite (2.2 g, 0.0315 mol) in water (10 mL). After stirring the mixture for 12 h at 15−20 °C, the compound **6** (5 g, 0.0263 mol) in one portion was added, followed by a portionwise addition of zinc dust (3.46 g, 0.0526 mol) maintaining the temperature below 15 °C. After completion of addition, zinc was allowed to react at room temperature with vigorous stirring for 15−20 min, and then the mixture was heated at 80 °C for 1.5 h. It was allowed to attain room temperature and then poured onto the ice cold water (∼500 mL). The precipitated off-white solid was isolated by filtration, dried, and recrystallized from

DOI: 10.1021/acs.joc.5b00654
J. Org. Chem. 2015, 80, 6152−6164

chloroform to give **7** as a white solid. Yield: 6.12 g, 90.5%; mp: 127 °C; ^{1}H NMR; (500 MHz; $CDCl_3$, TMS): δ 1.35 (t, J = 7 Hz, 3H), 2.18 (s, 3H), 2.22 (s, 3H), 3.76 (s, 2H), 4.3 (q, J = 7.5 Hz, 2H) 7.09−7.17 (m, 3H), 7.25 (t, J = 7.5 Hz, 2H), 8.63 (s, 1H); ^{13}C NMR; (500 MHz; $CDCl_3$, TMS): δ 10.8, 11.9, 14.6, 29.8, 59.7, 117.0, 120.3, 125.7, 128.0, 128.3, 130.1, 141.2, 161.6; MS (ESI): m/z calcd for $(M + H)^+$ $C_{16}H_{20}NO_2$ 258.1; found 257.9.

Synthesis of Sodium 4-Benzyl-3,5-dimethyl-1*H*-pyrrole-2-carboxylate (8). To a solution of **7** (5 g, 0.0194 mol) in ethanol (20 mL) was added sodium hydroxide (1.55 g, 0.0388 mol), followed by ∼0.5 mL of water. The resulting mixture was allowed to stir at reflux temperature for 5 h. After completion of reaction, confirmed by TLC, the reaction mixture allowed to cool to r.t. The excess ethanol was removed under vacuum, and the white solid product was isolated after filtration, dried, and washed with a little ice cold water, followed by 5% ethyl acetate in pet ether, which yielded **8** in the pure form as a white solid (4.62 g, 94.6%); ^{1}H NMR (500 MHz; D_2O, TMS): δ 2.03 (s, 3H), 2.04 (s, 3H), 3.56 (s, 2H), 7.04−7.08 (m, 3H), 7.18 (t, J = 7.5 Hz, 2H); ^{13}C NMR (500 MHz; $CDCl_3$, TMS): δ 11.1, 11.3, 31.1, 118.0, 120.3, 124.2, 124.3, 125.8, 128.4, 128.5, 142.8, 167.7; HRMS (ESI): m/z calcd for $(M - 23)^+$ $C_{14}H_{14}NO_2^-$ 228.1030; found 228.0155.

Synthesis of 3-Benzyl-2,4-dimethyl-1*H*-pyrrole (9). To the compound **8** (4 g, 0.0159 mol) in a 50 mL round-bottom flask was added trifluoroacetic acid (8 mL) at 20 °C under a N_2 atmosphere and stirred for 5 min. Then, to this was added 20 mL of chloroform, and the mixture was immediately washed with cold water, followed by twice with saturated sodium bicarbonate solution. Then, the organic layer was dried on sodium sulfate, and the solvent was evaporated, which, upon cooling, furnished **9** as an off-white to light brown solid (1.8 g, 61%), which was stored in a refrigerator and used for the next step without further purification.

^{1}H NMR (500 MHz; $CDCl_3$, TMS): δ 1.96 (s, 3H), 2.18 (s, 3H), 3.78 (s, 2H), 6.44 (s, 1H), 7.16 (d, J = 7.5 Hz, 3H), 7.20−7.24 (m, 2H), 7.61 (s, 1H); ^{13}C NMR (500 MHz; $CDCl_3$, TMS): δ 10.6, 11.5, 30.2, 113.0, 125.3, 125.4, 126.4, 128.1, 128.2, 128.2, 142.3; IR: cm^{-1} 3415, 1604, 1490, 1452, 1351, 1226, 1155; MS (ESI): m/z calcd for $(M + H)^+$ $C_{13}H_{16}N$ 186.1; found 186.3.

Synthesis of 4-Benzyl-3,5-dimethyl-1*H*-pyrrole-2-carbaldehyde (10). The compound **10** was synthesized from its corresponding precursors following the procedure reported in ref 18; Yield = 90.6%; ^{1}H NMR (500 MHz; $CDCl_3$, TMS): δ 2.22 (s, 3H), 2.24 (s, 3H), 3.78 (s, 2H), 7.11 (d, J = 7.5 Hz, 2H), 7.18 (t, J = 7.5 Hz, 1H), 7.27 (t, J = 7.5 Hz, 2H), 9.45 (s, 1H), 9.80 (bs, 1H); ^{13}C NMR(500 MHz; $CDCl_3$, TMS): δ 9.0, 12.1, 29.6, 126.0, 126.4, 126.5, 127.8, 127.9, 128.0, 128.5, 128.6, 173.9; HRMS (ESI): m/z calcd for $(M + H)^+$ $C_{14}H_{16}NO$ 214.1234; found 214.1218.

Synthesis of 2,6-Dibenzyl-4,4-difluoro-1,3,5,7,8-pentamethyl-4-bora-3a,4a-diaza-*s*-indecene (2). The compound **9** (200 mg, 1.08 mmol) was dissolved in 100 mL of dry dichloromethane, and the mixture was degassed for 10 min using dry nitrogen. Then, to this was added 38.5 μL (0.54 mmol) of acetyl chloride under a N_2 atmosphere. The resulting mixture was allowed to stir at room temperature for 4 h. Then, the dichloromethane was removed under vacuum to dryness, and the obtained dark red solid was washed twice with *n*-hexane (15 mL × 2). The dried solid was again dissolved in fresh dichloromethane (100 mL), followed by dropwise addition of 2.5 mL of triethyl amine. The reaction mass was allowed to stir for 10 min at room temperature, and then to this was added 3 mL of BF_3:OEt_2 dropwise over 5 min under a N_2 atmosphere at r.t. The resulting reaction mixture was stirred for 1 h at room temperature and then washed with water, followed by 1 N NaOH ice cold solution. The organic layer was separated, dried over sodium sulfate, and concentrated under vacuum, and the obtained dark red colored solid was then subjected to silica gel column chromatography using 0.5−1% ethyl acetate in hexane, which yielded 88 mg of a dark orange colored solid. Yield = 18.4%; ^{1}H NMR (500 MHz, $CDCl_3$, TMS): δ 2.34 (s, 6H), 2.47 (s, 6H), 2.65 (s, 3H), 3.81 (s, 4H), 7.11 (d, J = 7.5 Hz, 4H), 7.19 (t, J = 7.5 Hz, 2H), 7.26−7.29 (m, 4H); ^{13}C NMR (500 MHz, $CDCl_3$, TMS): δ 12.8, 18.9, 17.1, 29.6, 126.0, 127.9, 128.5, 128.8, 131.9, 137.8, 140.0, 140.5, 152.9; ^{19}F NMR (500 MHz, $CDCl_3$, TMS): δ −145.87 (q, J = 35.5 Hz). HRMS (ESI): m/z calcd for $(M + H)^+$ $C_{28}H_{30}BF_2N_2$ 443.2472; found 443.2451.

Synthesis of 2,6-Dibenzyl-4,4-difluoro-1,3,5,7-tetramethyl-8-phenyl-4-bora-3a,4a-diaza-*s*-indecene (3). Following the similar procedure as described for the dye **2**, the dye **3** (96 mg) was prepared from compound **9** (200 mg, 1.08 mmol) and benzoyl chloride (38.5 μL, 0.54 mmol). Yield = 17.6%; ^{1}H NMR(500 MHz, $CDCl_3$, TMS): δ 1.29 (s, 6H), 2.50 (s, 6H), 3.70 (s, 4H), 7.06 (dd, J = 7.5 Hz and J = 1 Hz, 4H), 7.16 (t, J = 7.5 Hz, 2H), 7.23−7.29 (m, 4H), 7.30−7.32 (m, 2H), 7.45−7.48 (m, 3H); ^{13}C NMR (500 MHz, $CDCl_3$, TMS): δ 12.1, 12.9, 29.6, 126.0, 128.0, 128.2, 128.4, 128.9, 129.1, 129.3, 131.0, 135.5, 139.8, 139.9, 140.9, 154.7; ^{11}B NMR (500 MHz, $CDCl_3$, TMS): δ 0.84 (t, J = 103 Hz); ^{19}F NMR (500 MHz, $CDCl_3$, TMS): δ −145.54 (q, J = 35 Hz); HRMS (ESI): m/z calcd for $(M + H)^+$ $C_{33}H_{32}BF_2N_2$ 505.2628; found 505.2631.

Synthesis of 2,6-Dibenzyl-4,4-difluoro-1,3,5,7-tetramethyl-8*H*-4-bora-3a,4a-diaza-*s*-indecene (4). The dye **4** was synthesized following the procedure reported in ref 18. Yield = 86.4%; ^{1}H NMR(500 MHz, $CDCl_3$, TMS): δ 2.17 (s, 6H), 2.45 (s, 6H), 3.78 (s, 4H), 7.05 (s, 1H), 7.12 (d, J = 7.5 Hz, 4H), 7.19 (t, J = 7.5 Hz, 2H), 7.26−7.29 (m, 4H); ^{13}C NMR (500 MHz, $CDCl_3$, TMS): δ 9.8, 12.9, 29.9, 119.2, 126.1, 128.0, 128.2, 128.5, 132.6, 138.1, 139.7, 155.7; ^{11}B NMR (500 MHz, $CDCl_3$, TMS): δ 0.9 (t, J = 103.5 Hz); ^{19}F NMR (500 MHz, $CDCl_3$, TMS): δ −146.06 (q, J = 35 Hz).HRMS (ESI): m/z calcd for $(M + H)^+$ $C_{27}H_{28}BF_2N_2$ 429.2315; found 429.2314.

■ ASSOCIATED CONTENT

Supporting Information

Mulliken charge density table, optimized geometry of the dyes, and schematic representation of the broad-band dye laser setup. Plausible reaction mechanisms of the dyes with singlet oxygen and DFT and TD-DFT data. ^{1}H and ^{13}C NMR, MS, and/HRMS spectra of the intermediates and dyes. The Supporting Information is available free of charge on the ACS Publications website at DOI: 10.1021/acs.joc.5b00654.

■ AUTHOR INFORMATION

Corresponding Authors

*E-mail: alokray@barc.gov.in (A.K.R.).
*E-mail: nethi.sekar@gmail.com (N.S.).

Notes

The authors declare no competing financial interest.

■ ACKNOWLEDGMENTS

Authors thank Mr. Amol Patil and Prof. B. M. Bhange, ICT, for their help in electrochemistry experiments. Also, we are thankful to Dr. V. Sudarshan, Chemistry Division, BARC, for his help in fluorescence lifetime decay measurements. K.G.T. is thankful to the Council of Scientific and Insdustrial Research (CSIR), India, for Junior and Senior Research Fellowships. R.M. is thankful to the UGC-CAS in Green Technology for the award of JRF and SRF under SAP.

■ REFERENCES

(1) (a) Paviopoulos, T. G.; Boyer, J. H.; Thangaraj, K.; Sathyamoorthi, G.; Shah, M. P.; Soong, M. L. *Appl. Opt.* **1992**, *31* (33), 7089−7094. (b) O'Neil, M. P. *Opt. Lett.* **1993**, *18* (1), 37.

(2) Haugland, R. P. *Handbook of Fluorescent Probes and Research Chemicals*, 6th ed.; Molecular Probes: Eugene, OR, 1996.

(3) Hattori, S.; Ohkubo, K.; Urano, Y.; Sunahara, H.; Nagano, T.; Wada, Y.; Tkachenko, N. V.; Lemmetyinen, H.; Fukuzumi, S. *J. Phys. Chem. B* **2005**, *109* (32), 15368−15375.

(4) (a) Rurack, K.; Kollmannsberger, M.; Resch-Genger, U.; Daub, J. *J. Am. Chem. Soc.* **2000**, *122* (5), 968−969. (b) Turfan, B.; Akkaya, E. U. *Org. Lett.* **2002**, *4* (17), 2857−2859. (c) Goze, C.; Ulrich, G.;

DOI: 10.1021/acs.joc.5b00654
J. Org. Chem. 2015, 80, 6152−6164

Charbonniere, L.; Cesario, M.; Prange, T.; Ziessel, R. *Chem.—Eur. J.* **2003**, *9* (16), 3748−3755. (d) Oleynik, P.; Ishihara, Y.; Cosa, G. *J. Am. Chem. Soc.* **2007**, *129* (7), 1842−1843. (e) Boens, N.; Leen, V.; Dehaen, W. *Chem. Soc. Rev.* **2012**, *41* (3), 1130−1172. (f) Bozdemir, O. A.; Guliyev, R.; Buyukcakir, O.; Selcuk, S.; Kolemen, S.; Gulseren, G.; Nalbantoglu, T.; Boyaci, H.; Akkaya, E. U. *J. Am. Chem. Soc.* **2010**, *132* (23), 8029−8036.

(5) Li, F.; Yang, S. I.; Ciringh, Y.; Seth, J.; Martin, C. H.; Singh, D. L.; Kim, D.; Birge, R. R.; Bocian, D. F.; Holten, D.; Lindsey, J. S. *J. Am. Chem. Soc.* **1998**, *120* (39), 10001−10017.

(6) Debreczeny, M. P.; Svec, W. A.; W, M. R. *Science* **1996**, *274* (5287), 584−587.

(7) (a) Dhokale, B.; Jadhav, T.; Mobin, S. M.; Misra, R. *Chem. Commun. (Cambridge, U.K.)* **2014**, *50* (65), 9119−9121. (b) Dhokale, B.; Jadhav, T.; Mobin, S. M.; Misra, R. *Dalton Trans.* **2015**, DOI: 10.1039/c5dt00565e. (c) Misra, R.; Jadhav, T.; Dhokale, B.; Gautam, P.; Sharma, R.; Maragani, R.; Mobin, S. M. *Dalton Trans.* **2014**, *43* (34), 13076−13086. (d) Misra, R.; Dhokale, B.; Jadhav, T.; Mobin, S. M. *New J. Chem.* **2014**, *38* (8), 3579. (e) Misra, R.; Dhokale, B.; Jadhav, T.; Mobin, S. M. *Dalton Trans.* **2014**, *43* (12), 4854−4861. (f) Misra, R.; Dhokale, B.; Jadhav, T.; Mobin, S. M. *Dalton Trans.* **2013**, *42* (37), 13658−13666. (g) Misra, R.; Dhokale, B.; Jadhav, T.; Mobin, S. M. *Organometallics* **2014**, *33* (7), 1867−1877. (h) Lu, H.; Mack, J.; Yang, Y.; Shen, Z. *Chem. Soc. Rev.* **2014**, *43* (13), 4778−4823. (i) Nepomnyashchii, A. B.; Bard, A. J. *Acc. Chem. Res.* **2012**, *45* (11), 1844−1853.

(8) (a) Pavlopoulos, T. G.; Boyer, J. H.; Shah, M.; Thangaraj, K.; Soong, M. L. *Appl. Opt.* **1990**, *29* (27), 3885−3886. (b) Guggenheimer, S. C.; Boyer, J. H.; Thangaraj, K.; Shah, M.; Soong, M. L.; Paviopoulos, T. G. *Appl. Opt.* **1993**, *32* (21), 3942−3943. (c) Boyer, J. H.; Haag, A. M.; Sathyamoorthi, G.; Soong, M.-L.; Thangaraj, K.; Pavlopoulos, T. G. *Heteroat. Chem.* **1993**, *4* (1), 39−49. (d) Duchowicz, R.; Scaffardi, L. B.; Costela, A.; García-Moreno, I.; Sastre, R.; Acuña, A. U. *Appl. Opt.* **2003**, *42* (6), 1029. (e) Pavlopoulos, T. G.; Shah, M.; Boyer, J. H. *Opt. Commun.* **1989**, *70* (5), 425−427.

(9) Jagtap, K. K.; Shivran, N.; Mula, S.; Naik, D. B.; Sarkar, S. K.; Mukherjee, T.; Maity, D. K.; Ray, A. K. *Chem.—Eur. J.* **2013**, *19* (2), 702−708.

(10) (a) Faloss, M.; Canva, M.; Georges, P.; Brun, A.; Chaput, F.; Boilot, J.-P. *Appl. Opt.* **1997**, *36* (27), 6760. (b) Costela, A.; Garcia-Moreno, I.; Sastre, R. *Phys. Chem. Chem. Phys.* **2003**, *5* (21), 4745. (c) Ray, A. K.; Kumar, S.; Mayekar, N. V.; Sinha, S.; Kundu, S.; Chattopadhyay, S.; Dasgupta, K. *Appl. Opt.* **2005**, *44* (36), 7814. (d) Lopez Arbeloa, F.; Banuelos Prieto, J.; Lopez Arbeloa, I.; Costela, A.; Garcia-Moreno, I.; Gomez, C.; Amat-Guerri, F.; Liras, M.; Sastre, R. *Photochem. Photobiol.* **2003**, *78* (1), 30−36.

(11) Rahn, M. D.; King, T. A.; Gorman, A. A.; Hamblett, I. *Appl. Opt.* **1997**, *36* (24), 5862.

(12) (a) Burghart, A.; Kim, H.; Welch, M. B.; Thoresen, L. H.; Reibenspies, J.; Burgess, K.; Bergström, F.; Johansson, L. B.-Å. *J. Org. Chem.* **1999**, *64* (21), 7813−7819. (b) Chen, J.; Burghart, A.; Derecskei-Kovacs, A.; Burgess, K. *J. Org. Chem.* **2000**, *65* (10), 2900−2906. (c) Goze, C.; Ulrich, G.; Mallon, L. J.; Allen, B. D.; Harriman, A.; Ziessel, R. *J. Am. Chem. Soc.* **2006**, *128* (31), 10231−10239. (d) Mula, S.; Ray, A. K.; Banerjee, M.; Chaudhuri, T.; Dasgupta, K.; Chattopadhyay, S. *J. Org. Chem.* **2008**, *73* (6), 2146−2154.

(13) Jones, G.; Kumar, S.; Klueva, O.; Pacheco, D. *J. Phys. Chem. A* **2003**, *107* (41), 8429−8434.

(14) *Solid State Lasers X*; San Jose, CA, 24−25 January, 2001; SPIE: Bellingham, WA, 2001; Vol. *4267*.

(15) Mula, S.; Ray, A. K.; Banerjee, M.; Chaudhuri, T.; Dasgupta, K.; Chattopadhyay, S. *J. Org. Chem.* **2008**, *73* (6), 2146−2154.

(16) Treibs, A.; Derra-Scherer, H. *Justus Liebigs Ann. Chem.* **1954**, *589* (3), 188−195.

(17) (a) Lehr, M. *J. Med. Chem.* **1997**, *40* (21), 3381−3392. (b) Battersby, A. R.; Baker, M. G.; Broadbent, H. A.; Fookes, C. J. R.; Leeper, F. J. *J. Chem. Soc., Perkin Trans. 1* **1987**, 2027.

(18) Wu, L.; Burgess, K. *Chem. Commun. (Cambridge, U.K.)* **2008**, *No. 40*, 4933−4935.

(19) Mula, S.; Elliott, K.; Harriman, A.; Ziessel, R. *J. Phys. Chem. A* **2010**, *114* (39), 10515−10522.

(20) Thorat, K. G.; Bhakhoa, H.; Ramasami, P.; Sekar, N. *J. Fluoresc.* **2015**, *25* (1), 69−78.

(21) Frisch, M. J.; Trucks, G. W.; Schlegel, H. B.; Scuseria, G. E.; Robb, M. A.; Cheeseman, J. R.; Scalmani, G.; Barone, V.; Mennucci, B.; Petersson, G. A.; Nakatsuji, H.; Caricato, M.; Li, X.; Hratchian, H. P.; Izmaylov, A. F.; Bloino, J.; Zheng, G.; Sonnenberg, J. L.; Hada, M.; Ehara, M.; Toyota, K.; Fukuda, R.; Hasegawa, J.; Ishida, M.; Nakajima, T.; Honda, Y.; Kitao, O.; Nakai, H.; Vreven, T.; Montgomery, J. A., Jr.; Peralta, J. E.; Ogliaro, F.; Bearpark, M.; Heyd, J. J.; Brothers, E.; Kudin, K. N.; Staroverov, V. N.; Kobayashi, R.; Normand, J.; Raghavachari, K.; Rendell, A.; Burant, J. C.; Iyengar, S. S.; Tomasi, J.; Cossi, M.; Rega, N.; Millam, J. M.; Klene, M.; Knox, J. E.; Cross, J. B.; Bakken, V.; Adamo, C.; Jaramillo, J.; Gomperts, R.; Stratmann, R. E.; Yazyev, O.; Austin, A. J.; Cammi, R.; Pomelli, C.; Ochterski, J. W.; Martin, R. L.; Morokuma, K.; Zakrzewski, V. G.; Voth, G. A.; Salvador, P.; Dannenberg, J. J.; Dapprich, S.; Daniels, A. D.; Farkas, Ö; Foresman, J. B.; Ortiz, J. V; Cioslowski, J.; Fox, D. J. *Gaussian 09*, C.01; Gaussian Inc.: Wallingford, CT, 2009.

(22) Treutler, O.; Ahlrichs, R. *J. Chem. Phys.* **1995**, *102* (1), 346.

(23) Becke, A. D. *J. Chem. Phys.* **1993**, *98* (2), 1372.

(24) Lee, C.; Yang, W.; Parr, R. G. *Phys. Rev. B* **1988**, *37* (2), 785−789.

(25) (a) Hehre, W. J. *Acc. Chem. Res.* **1976**, *9* (11), 399−406. (b) Bauernschmitt, R.; Ahlrichs, R. *Chem. Phys. Lett.* **1996**, *256* (4−5), 454−464. (c) Furche, F.; Rappoport, D. *Computational Photochemistry (Google eBook)*; Olivucci, M., Ed.; Elsevier: Amsterdam, 2005. (d) Gabe, Y.; Ueno, T.; Urano, Y.; Kojima, H.; Nagano, T. *Anal. Bioanal. Chem.* **2006**, *386* (3), 621−626. (e) Furche, F.; Ahlrichs, R. *J. Chem. Phys.* **2002**, *117* (16), 7433. (f) Leszczynski, J., Shukla, M., Eds. *Practical Aspects of Computational Chemistry: Methods, Concepts and Applications (Google eBook)*; Springer: Heidelberg, Germany, 2009. (g) Scalmani, G.; Frisch, M. J.; Mennucci, B.; Tomasi, J.; Cammi, R.; Barone, V. *J. Chem. Phys.* **2006**, *124* (9), 94107.

(26) (a) Cossi, M.; Barone, V.; Cammi, R.; Tomasi, J. *Chem. Phys. Lett.* **1996**, *255* (4−6), 327−335. (b) Tomasi, J.; Mennucci, B.; Cammi, R. *Chem. Rev.* **2005**, *105* (8), 2999−3093.

DOI: 10.1021/acs.joc.5b00654
J. Org. Chem. 2015, 80, 6152−6164